

CYCLIC AMP REGULATES AN INWARD RECTIFYING SODIUM-POTASSIUM CURRENT IN DISSOCIATED BULL-FROG SYMPATHETIC NEURONES

BY T. TOKIMASA AND T. AKASU

*From the Department of Physiology, Kurume University School of Medicine,
67 Asahi-machi, Kurume 830, Japan*

(Received 17 April 1989)

SUMMARY

1. Bull-frog sympathetic neurones in primary culture were voltage clamped in the whole-cell configuration. The pipette solution contained ATP (5 mM).

2. A hyperpolarization-activated sodium-potassium current (H-current: I_H) was separated from other membrane currents in a nominally calcium-free solution containing cobalt (2 mM), magnesium (4 mM), barium (2 mM), tetraethylammonium (20 mM), tetrodotoxin (3 μ M), apamin (30 nM) and 4-aminopyridine (1 mM). I_H was selectively blocked by caesium (10–300 μ M).

3. The steady-state activation of I_H occurred between -60 and -130 mV. The H-conductance was 4.1–6.6 nS at the half-activation voltage of -90 mV. With the concentrations of potassium and sodium ions in the superfusate at 20 and 70 mM, respectively, the reversal potential of I_H was about -20 mV. I_H was activated with a time constant of 2.8 s at -90 mV and 22 °C. The Q_{10} between 16 and 26 °C was 4.3.

4. A non-hydrolysable ATP analogue in the pipette solution did not support I_H activation. Intracellular 'loading' of GTP- γ -S (30–500 μ M) led to a progressive activation of I_H .

5. Forskolin (10 μ M) increased the maximum conductance of I_H by 70%. This was associated with a depolarizing shift in the half-activation voltage (5–10 mV) and in the voltage dependence of the activation/deactivation time constant of I_H .

6. Essentially the same results as with forskolin were obtained by intracellular 'loading' with cyclic AMP (3–10 μ M) or bath application of 8-bromo cyclic AMP (0.1–1 mM), dibutyryl cyclic AMP (1 mM) and 3-isobutyl-1-methylxanthine (0.1–1 mM).

7. The protein kinase inhibitor H-8 (1–10 μ M) decreased the peak amplitude of I_H . Phorbol 12-myristate 13-acetate (10 μ M), a protein kinase C activator, was without effect.

8. It is concluded that a voltage-dependent cation current can be regulated by the basal activity of adenylate cyclase, presumably through protein kinase A, in vertebrate sympathetic neurones.

INTRODUCTION

A hyperpolarization-activated sodium-potassium current (H-current: I_H) appears to occur in a variety of vertebrate nerve cells (Barrett, Barrett & Crill, 1980; Halliwell & Adams, 1982; Mayer & Westbrook, 1983; Crepel & Penit-Soria, 1986; Griffith, 1988; Williams, Colmers & Pan, 1988*a*). However, the intracellular control mechanisms have not yet been described for this cation current.

The main purpose of the present study was to investigate the intracellular mechanisms for I_H in bull-frog sympathetic neurones in a primary culture. The results show that I_H could be regulated by the basal activity of adenylate cyclase. A preliminary account of portions of the present study has appeared in abstract form (Tokimasa, Akasu, Nishimura & Tsurusaki, 1989).

METHODS

All the experiments in the present study were carried out at 22–24 °C except the determination of the Q_{10} for I_H . The statistics are expressed as means \pm s.e. of the means (s.e.m.). The pH of the superfusate was adjusted to 7.2.

Tissue culture. Small (200–250 g) bull-frogs (*Rana catesbeiana*) were used. After decapitation and pithing, paravertebral sympathetic ganglia were rapidly dissected, de-sheathed and minced with forceps into small pieces (Kuffler & Sejnowski, 1983). These fragments were incubated with gentle pipetting or stirring at room temperature (22–24 °C) for 30 min in Ringer solution containing 0.5 mg ml⁻¹ collagenase (Sigma type I) and 2.5 mg ml⁻¹ trypsin (Sigma type XI). The Ringer solution had the following composition (mM): NaCl, 112; KCl, 2; CaCl₂, 1.8; *N*-2-hydroxyethylpiperazine-*N'*-2-ethanesulphonic acid (HEPES), 4 and tris(hydroxymethyl)aminomethane (TRIS), 1. The enzymatic digestion was repeated up to ten times. After each digestion, the dissociated cells were collected by centrifugation (80 g for 5 min) and stocked for 2–10 days at 4 °C in Leibovitz's L-15 medium (GIBCO 320-1415; 10–20% fetal bovine serum (FBS: GIBCO 200-6140AG) added and then diluted to 80% with H₂O) in 35 mm plastic culture dishes (Falcon 3001). Penicillin/streptomycin (GIBCO 600-5140) (0.1 mg ml⁻¹) was added to L-15 medium.

I_H could be detected even in acutely dissociated cells but only when they were stocked in L-15 medium for 3 h or longer. This might have resulted from damage of membrane proteins such as those responsible for ionic channels caused by digestive enzymes. The possible mechanisms of these phenomena have not been examined in the present study and we simply used those cells stocked in the culture medium for more than 24 h.

Whole-cell clamp. The cultured cells were resuspended in Ringer solution about 2 h prior to the electrophysiological experiments. The cells were pipetted into the recording chamber (1.5 ml total volume) which was continuously superfused (1–3 ml min⁻¹) with Ringer solution.

Pipettes for the whole-cell clamp had a tip resistance of 3–6 M Ω when they were filled with a pipette solution having the following composition (mM): KCl, 100; ethylene glycol-bis(β -aminoethyl ether)*N,N,N'*-tetraacetic acid (EGTA), 1; adenosine 5'-triphosphate disodium (Na₂ATP), 5; MgCl₂, 4; and HEPES (sodium salt), 2.5 (pH adjusted with KOH to 7.0–7.1) (see Jones, 1987*b*). A sample-and-hold voltage-clamp amplifier (Axoclamp-2A) was used to measure the whole-cell currents (9–15 kHz switching frequency with a 70–30 duty cycle).

The dissociated cells were photographed and the photoprints were used to measure the soma size. The soma size of each cell was determined by measuring its major and minor axes and was expressed by a mean diameter defined as the square root of the multiple of these axes. The mean diameter of the cells used in the present study ranged from 37 to 47 μ m. In nine cells having the mean diameter of 43 μ m, the average cell capacitance was 83 \pm 9 pF, determined from the time constant and input resistance from charging curves at hyperpolarized potentials (2 mM-caesium present in the bath). This corresponds to a specific membrane capacitance of 1.17 \pm 0.2 μ F cm⁻² (see Jones, 1987*a*). It would be reasonable to assume that a surface area of those cells having the mean diameter of 43 μ m may amount to 58 \times 10⁻⁶ cm² and hence a total membrane current of 1 nA would be equivalent to about 17 μ A cm⁻².

In all of ten cells, muscarine (1–10 μ M) depressed the amplitude of the M-current (Adams, Brown

& Constanti, 1982*a, b*) and depolarized the membrane indicating that B-cells were used in the present study (Dodd & Horn, 1983).

Standard solution for I_H . The properties of I_H were studied in a nominally calcium-free solution with the following composition (mM unless otherwise stated): NaCl, 70; KCl, 20; CoCl₂, 2; MgCl₂, 4; BaCl₂, 2, tetraethylammonium, 20; tetrodotoxin, (3 μ M); apamin (30 nM); 4-aminopyridine, 1; HEPES, 4 and TRIS, 1. This is the 'standard' solution.

Drugs. The drugs used (from Sigma) were β - γ -imidoadenosine 5'-triphosphate (APP(NH)P), adenosine 3',5'-cyclic monophosphate (sodium salt), adenosine 5'-triphosphate (disodium salt), 8-bromoadenosine 3',5'-cyclic monophosphate (sodium salt), N⁶,2'-O-dibutyryl adenosine 3',5'-cyclic monophosphate (sodium salt), guanosine 3',5'-cyclic monophosphate (sodium salt), guanosine 5'-O-(3-thiotriphosphate) (tetralithium salt), guanosine 5'-O-(2-thiodiphosphate) (trilithium salt), apamin, DL-muscarine chloride, phorbol 12-myristate 13-acetate, forskolin and 4-aminopyridine. Other drugs used were tetrodotoxin (Sankyo), islet-activating protein (Kaken Pharmaceutical), luteinizing hormone-releasing hormone (Peptide Institute), protein kinase inhibitor H-8 (Seikagaku Kogyo), and 3-isobutyl-1-methylxanthine (Aldrich). Phorbol 12-myristate 13-acetate (PMA) was dissolved with dimethyl sulphoxide (Wako Pure Chemicals) (3.3 mg ml⁻¹) and stored at -20 °C.

RESULTS

Potentials were recorded from bull-frog sympathetic neurones in primary cultures ($n > 150$). The resting membrane potential of the cells was -63 ± 1 mV about 5 min after rupturing the membrane patch ($n = 130$; range from -54 to -70 mV). The peak amplitude of the action potentials evoked by brief (8–10 ms) depolarizing current pulses was 120 ± 3 mV ($n = 90$). The steady-state current–voltage (I – V) curve, measured at the end of prolonged (4.9 s) command steps from a holding potential of -30 mV, demonstrated an outward rectification between -30 and -60 mV (Fig. 1*A*). The rectification was due to a time- and voltage-dependent potassium current, the M-current (I_M) (Adams *et al.* 1982*a*).

Inward rectification

At potentials more negative than -65 mV, a de-activating I_M was followed by slowly developing inward relaxations on the current trace which were clearly detected at -90 and -100 mV (Fig. 1*B*). Inward relaxations on a current trace in response to step hyperpolarizations and the resultant inward rectification on the steady-state I – V curve were much more easily detected in a potassium-rich (20 mM) Ringer solution (Fig. 1*C* and *D*). The control current trace in Fig. 1*D* was not associated with an inward relaxation at -61 mV, whereas it clearly was at -87 mV implying that the threshold of this hyperpolarization-induced current relaxation lies between -61 and -87 mV. Caesium (1 mM) reversibly blocked the hyperpolarization-induced relaxations on the current trace (Fig. 1*C* and *D*). In these conditions, the steady-state I – V curve showed a negative slope between -48 and -65 mV and a positive slope at potentials negative to -65 mV (Fig. 1*C*). The negative slope conductance was eliminated by adding muscarine (3 μ M) ($n = 1$) and barium (1 mM) ($n = 2$) to the caesium-containing solution. Therefore, it was confirmed that the negative slope results from a hyperpolarization-induced deactivation of the steady inward flow of I_M between -48 and -65 mV (Adams *et al.* 1982*a*).

As described below, inward rectification is due to a hyperpolarization-activated sodium–potassium current and therefore this cation current is referred to as the H-current (I_H).

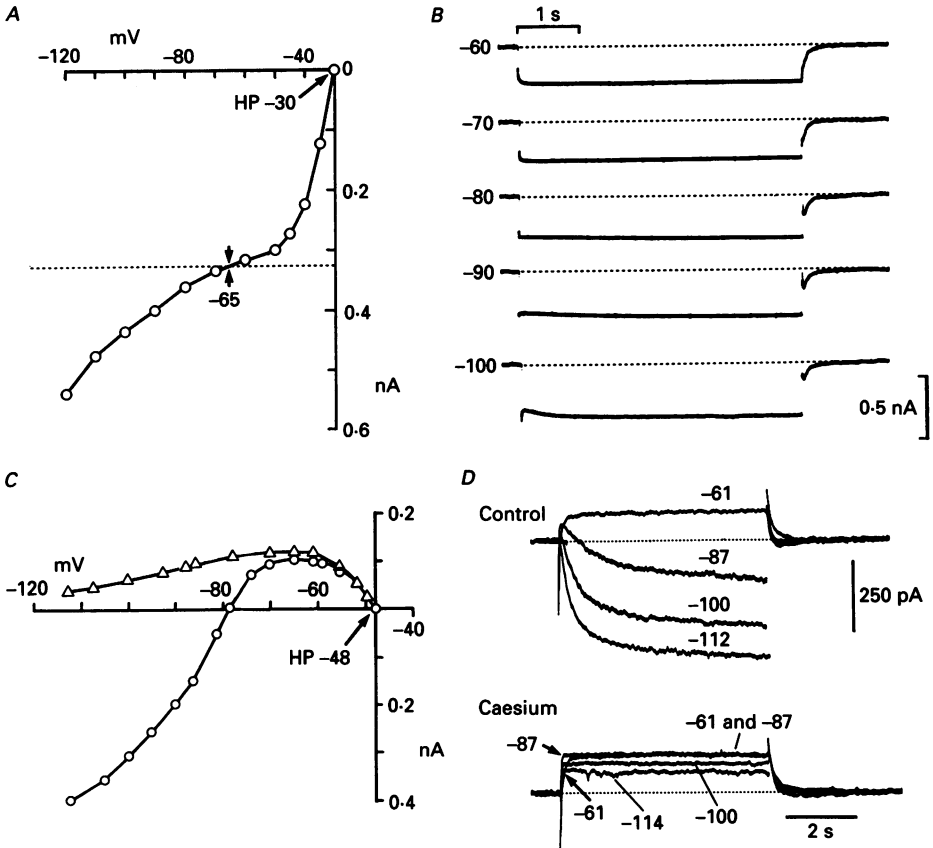


Fig. 1. I_H in dissociated bull-frog sympathetic neurones. Results in *A, B* ($2 \text{ mM } [K]_o$) and *C, D* ($20 \text{ mM } [K]_o$) were obtained from two cells. *A*, the steady-state $I-V$ curve in the normal Ringer solution, measured at the end of prolonged (4.9 s) command steps from the holding potential (HP) of -30 mV . The dotted line denotes the zero holding current level at the resting potential of -65 mV (indicated by arrows). *B*, sample recordings that were plotted in *A*. *C*, the steady-state $I-V$ curve in a potassium-rich Ringer solution, measured at the end of prolonged (6 s) hyperpolarizing step commands from a HP of -48 mV . \circ , the control $I-V$ curve; \triangle , the relationship in the presence of caesium (1 mM). *D*, sample recordings that were plotted in *C*. Commanding levels are indicated beside each trace. In *C* and *D*, membrane hyperpolarizations caused a deactivation of the steady-state inward flow of potassium current through the M-channels and thereby produced the negative slope conductance between -48 and -65 mV . Note that the negative slope was not blocked by caesium. Outward tail currents due to the reactivating I_M are seen on repolarization to -48 mV , both in control and in the presence of caesium. Arrows in the lower trace in *D* indicate the deactivating I_M which had a slower time course at -61 mV than at -87 mV . In this and the following figures, TTX ($1-3 \mu\text{M}$) was present throughout, unless otherwise mentioned.

Pharmacological isolation of I_H

In this and the following sections, a nominally calcium-free standard solution (see Methods for its composition) was used to isolate I_H from other membrane currents (see below).

TTX ($3 \mu\text{M}$) was used to block an inward sodium current (Jones, 1987a). Calcium ions were removed from and magnesium (4 mM), cobalt (2 mM) and apamin (30 nM) were added to the superfusate to eliminate an inward calcium current and subsequently activated potassium currents (Tokimasa, 1984, 1985a, b; Pennefather, Lancaster, Adams & Nicoll, 1985; Fox, Nowycky & Tsien, 1987; Tanaka & Kuba, 1987). TEA (20 mM) was used to reduce the amplitude of a classical delayed rectifier potassium current (Adams *et al.* 1982a). Barium (2 mM) was used to block I_{M} (Adams *et al.* 1982a, b). 4-AP (1 mM) was used to reduce the amplitude of the A-current (Adams *et al.* 1982a). The potassium concentration ($[\text{K}^+]_{\text{o}}$) was elevated to 20 mM so as to increase the amplitude of I_{H} (Fig. 1) (Halliwell & Adams, 1982; Mayer & Westbrook, 1983). In these conditions, almost all membrane currents, with the exceptions of I_{H} and a chloride current, were totally, or at least substantially, blocked.

A typical inward rectification in the steady-state I - V curve and the underlying I_{H} present in the standard solution are shown in Fig. 2. The main effects of changing the superfusate from the Ringer solution to the standard solution was to eliminate I_{M} by 2 mM -barium and to increase the amplitude of I_{H} by 20 mM -potassium. The latter effect masked a decrease in the amplitude of I_{H} by reducing $[\text{Na}^+]_{\text{o}}$ from 112 to 70 mM (see further below). Inward relaxations on the current trace during 70 mV and 80 mV hyperpolarizations from the holding potential of -30 mV were not affected by muscarine ($3 \mu\text{M}$) (Fig. 2D). This indicated that I_{M} has already been eliminated by 2 mM -barium and that I_{H} is insensitive to muscarine.

I_{H} was selectively and reversibly blocked when caesium (1 - 2 mM) was added to the standard solution (Fig. 3). Chord conductance between -50 and -110 mV was about 1.2 nS (range 0.5 - 4.0 nS ; $n = 10$) when I_{H} was blocked by caesium (1 - 2 mM) indicating the leak conductance in the absence of I_{H} (Fig. 3A). With the caesium concentration in the standard solution at 10 - 300 nM , the caesium-induced blockade of I_{H} was clearly voltage dependent. Caesium (10 nM) reduced the amplitude of I_{H} to about 60% at -130 mV but only to about 95% at -70 mV ($n = 3$). Such voltage-dependent block became less prominent in a concentration-dependent manner when the concentration of caesium was increased to 30 - 300 nM . Rubidium (1 - 5 mM) was also effective in reducing the amplitude of I_{H} although 3 mM -rubidium was about one-third as potent as 1 mM -caesium ($n = 3$) (Fig. 3C) (see Williams, North & Tokimasa, 1988b).

Voltage dependence of I_{H}

Reversal potential

The instantaneous I - V curves, measured at the onset of step hyperpolarizations from potentials at which I_{H} is absent (e.g. -35 mV in Fig. 4A, B) and at the onset of step depolarizations from potentials at which I_{H} is present (e.g. -93 mV in Fig. 4A and B), were linearly related to the membrane potential (Fig. 4A). The slopes of the I - V curves, 2.16 and 7.14 nS respectively, denote the leak conductance at -35 mV and the leak conductance plus the H-conductance at -93 mV . Extrapolations of the two straight lines in Fig. 4A intersected at -24 mV indicating the reversal potential of I_{H} (E_{H}). E_{H} was thus estimated as $-20.2 \pm 1.5 \text{ mV}$ ($n = 8$), $-31.3 \pm 1.4 \text{ mV}$ ($n = 6$), $-39.4 \pm 1.6 \text{ mV}$ ($n = 5$) and $-54.1 \pm 4.0 \text{ mV}$ ($n = 3$) when $[\text{K}^+]_{\text{o}}$ was 20 , 10 , 5 and 2 mM , respectively. Extracellular sodium concentration was maintained at 70 mM by substituting equimolar KCl with choline chloride (Fig. 4C). The relationship

between E_H and $\log [K^+]_o$ had a slope of 30 mV for a one decade change in $[K^+]_o$ (Fig. 4C).

Fully activated $I-V$ curve ($\bar{I}_{H(E)}$)

$\bar{I}_{H(E)}$ was obtained by the method described by DiFrancesco, Ferroni, Mazzanti & Tromba (1986). There was not a strong rectification of $\bar{I}_{H(E)}$ between -90 and

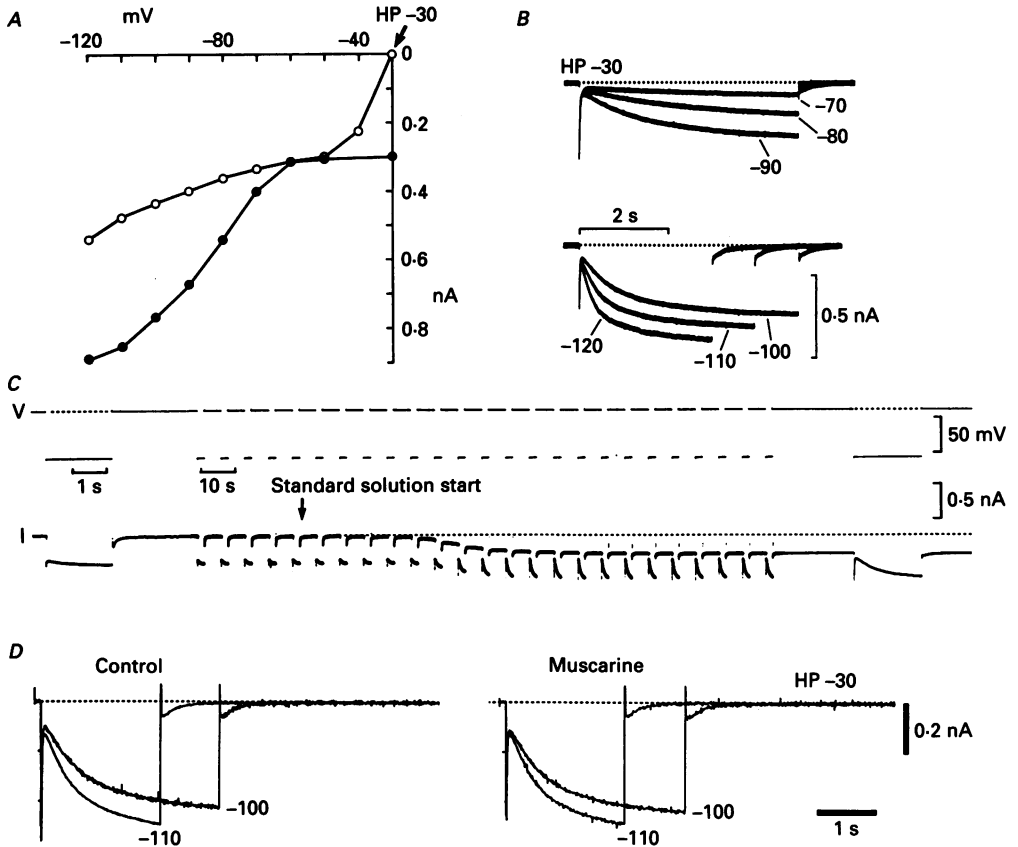


Fig. 2. Pharmacologically isolated I_H in the standard solution. Data in A–D were obtained from the same cell as that in Fig. 1A and B. A, the steady-state $I-V$ curve in Ringer solution (\circ) and in 'standard' solution (\bullet) measured at the end of prolonged (4.9 s) hyperpolarizing step commands from the holding potential (HP) of -30 mV. B, sample recordings that were plotted in A. The commanding levels are indicated beside each trace. C, effect of the 'standard' solution on the holding current at -30 mV. The step commands hyperpolarized the membrane to -100 mV for 2 s. The superfusate was changed from the normal Ringer solution to the 'standard' solution at the time indicated by the arrow. D, bath application of muscarine ($3 \mu\text{M}$) did not affect I_H at both -100 and -110 mV. The holding current at HP -30 mV did not show any inward shift in the presence of muscarine.

-10 mV, indicating that fully opened H-channels lack intrinsic voltage dependence ($n = 4$) (Fig. 4D). I_H was reversibly reduced in amplitude in all of six cells when $[\text{Na}]_o$ was reduced from 70 to 35 mM (choline chloride was substituted for NaCl) (Fig. 4E). $\bar{I}_{H(E)}$ displayed a hyperpolarizing shift along the voltage axis by 3–8 mV ($n = 3$) (Fig. 4D). $\bar{I}_{H(E)}$ in a sodium-free 'standard' solution had only a slightly smaller slope than

in control (Fig. 4D). These observations indicated that the main effects of changing $[\text{Na}^+]_o$ was to shift the I - V relationship of I_H . This is compatible with a previous study on the f-current in heart muscle cells (DiFrancesco *et al.* 1986).

I_H was not abolished in a nominally sodium-free 'standard' solution in all of three cells tested (Fig. 4E). The remaining current relaxations were readily blocked by caesium (1 mM) and therefore identified as the remaining I_H (not shown).

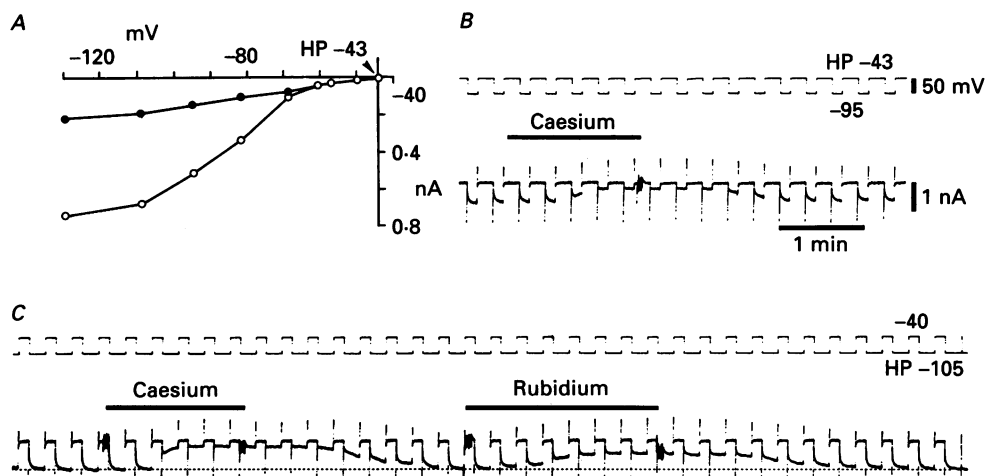


Fig. 3. Blockade of I_H by caesium and rubidium. The results in A-C were obtained from the same cell at the holding potential (HP) of -43 mV in A and B and at -105 mV in C. A, the steady-state I - V curves, measured at the end of step hyperpolarizations lasting for 5 s, in the standard solution ('control', \circ) and in the standard solution containing 1 mM-caesium (\bullet). B, the effects of caesium (1 mM) on I_H at -95 mV and the holding current at HP -43 mV. The holding current did not show an outward shift. C, the effects of caesium (1 mM) and rubidium (3 mM) on I_H at HP -105 mV. I_H was deactivated during step depolarizations from -105 to -40 mV and reactivated on stepping back to -105 mV. The holding current at -105 mV showed an outward shift during bath application of caesium and rubidium.

Steady-state activation curve

The steady-state activation curve of I_H was studied by plotting the peak amplitude of the inward tail current, after the termination of hyperpolarizing step commands, as a function of membrane potential (Fig. 5). The curve was described (least-squares method) by

$$I/I_{\max} = (1 + \exp((V_0 - V)/k))^{-1}, \quad (1)$$

where V is the membrane potential. I and I_{\max} , respectively, denote the amplitude of the deactivating tail current and its maximum value. I_{\max} was obtained between -120 and -130 mV. V_0 and k denote a half-activation voltage and the slope factor. V_0 and k were -90 mV and 8.7 mV (mean value from six cells in 90 mM $[\text{Na}^+]_o$ and 20 mM $[\text{K}^+]_o$) (Fig. 5A), and -91.0 ± 3.9 mV and 7.6 ± 0.5 mV ($n = 3$ in 70 mM $[\text{Na}^+]_o$ and 20 mM $[\text{K}^+]_o$) (Fig. 5B). V_0 and k were relatively independent of $[\text{K}^+]_o$ (Fig. 5B and C).

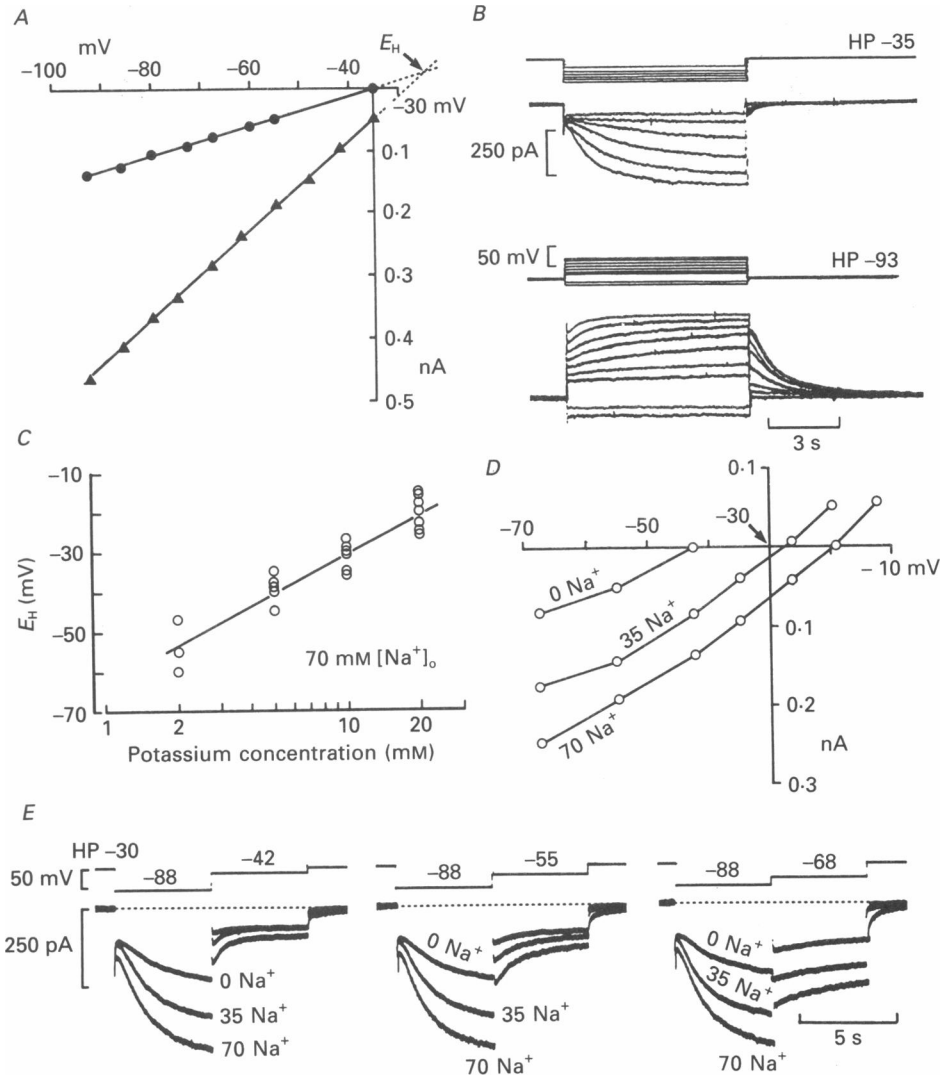


Fig. 4. The reversal potential and the fully activated $I-V$ curve of I_H . *A*, chord conductance measured instantaneously at the onset of hyperpolarizing step commands from a holding potential (HP) of -35 mV (\bullet ; slope 2.16 nS) and at the onset of depolarizing step commands from a HP of -93 mV (\blacktriangle ; slope 7.14 nS). Extrapolations of the two straight lines intersected at -24 mV (arrow). *B*, sample recordings which were plotted in *A*. *C*, the relationship between the reversal potential of I_H (E_H) (ordinate in mV) and $\log [K^+]_o$ (abscissa in mM). The $[Na^+]_o$ was 70 mM throughout. Each circle denotes the E_H in each cell. The straight line denotes the regression line (least-squares method), which had a slope of 30 mV for a one decade change in $[K^+]_o$. *D* and *E*, data from another cell in which the fully activated $I-V$ curve of I_H ($\bar{I}_{H(E)}$) was measured by the method used by DiFrancesco (1986). *D*, $\bar{I}_{H(E)}$ in 70 , 35 mM and zero $[Na^+]_o$ (indicated beside each $I-V$ curve). *E*, I_H in response to three different twin-pulse protocols in three different $[Na^+]_o$. The initial hyperpolarizing steps were from a HP of -30 to -88 mV for 5 s. The voltage levels during the second pulses were -42 (left), -55 (middle) and -68 mV (right). The $[Na^+]_o$ is indicated beside each current trace.

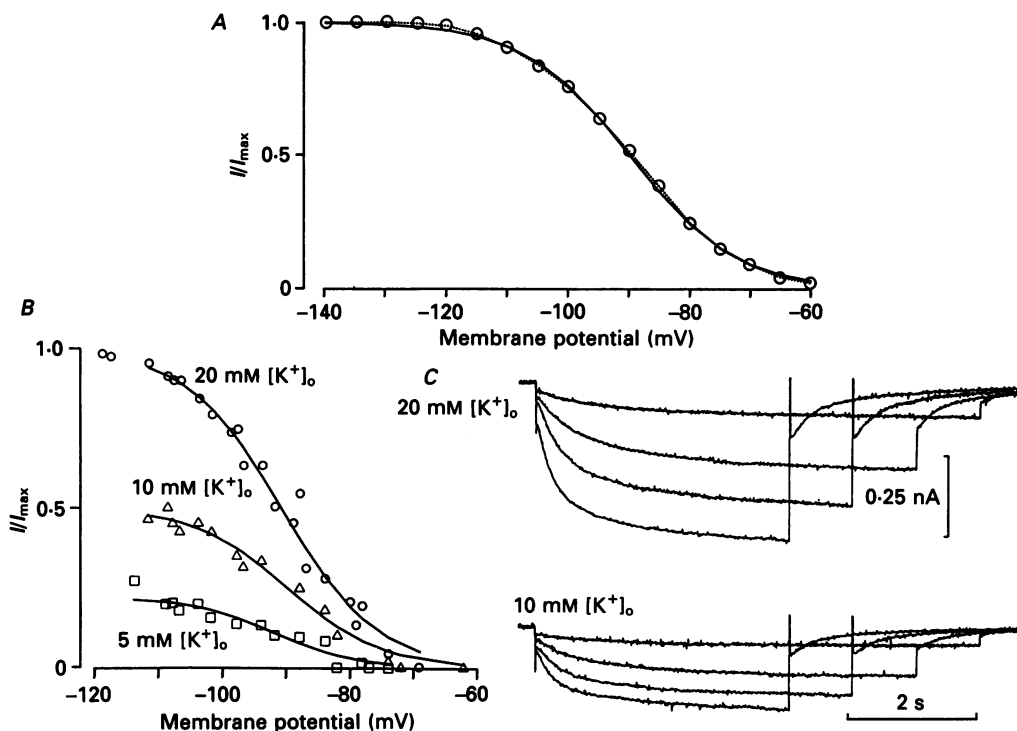


Fig. 5. Steady-state activation curve of I_H . In *A* and *B*, the relative amplitude of the inward tail current (I/I_{\max}) of I_H was plotted on the ordinate as a function of membrane potential (abscissa in mV). *A*, experiments in 20 mM $[K^+]_o$ and 90 mM $[Na^+]_o$. \circ , mean values of I/I_{\max} in six cells. A dotted line was drawn through the circles. The continuous line represents eqn (1) having -90 mV as V_0 and 8.7 mV as k . *B*, pooled data from three cells in 70 mM $[Na^+]_o$ and in three different $[K^+]_o$ (indicated beside each curve). I_{\max} at -120 mV in 20 mM $[K^+]_o$ was taken as 1.0. The continuous lines denote eqn (1). V_0 and k were, respectively, -92 and 6.7 mV for 5 mM $[K^+]_o$, -90 and 7.5 mV for 10 mM $[K^+]_o$, and -91 and 7.6 mV for 20 mM $[K^+]_o$. *C*, sample recordings from one of the three cells that was plotted in *B* (upper traces for 20 mM $[K^+]_o$ and lower traces for 10 mM $[K^+]_o$). The HP was -58 mV. The command levels were -78 , -88 , -98 and -108 mV in both 10 and 20 mM $[K^+]_o$.

The steady-state H-conductance (G_H) was calculated from the peak amplitude of the deactivating tail current of I_H and the driving force for I_H (the E_K minus a holding potential). At the half-activation voltage, G_H ranged from 4.1 to 6.6 nS ($n = 7$). I_H was eliminated in the potassium-free 'standard' solution ($n = 5$).

Time course of activation and deactivation

The time constant of the final exponential development of I_H (τ_{on}) could be described by $\tau_{on}^{-1} = (0.124(V + 120))/(1 + \exp((V + 120)/12)) + 0.003$, where V denotes membrane potential (see Yanagihara & Irisawa, 1980) (from the pooled data in eight cells). This indicates that τ_{on}^{-1} is increased e-fold by a 12 mV hyperpolarization (Fig. 6*A* and *B*). An envelope test (Yanagihara & Irisawa, 1980; Mayer & Westbrook, 1983; DiFrancesco *et al.* 1986) was used to study the time course of the deactivating I_H . τ_{off}^{-1}

was increased e-fold by a 16 mV depolarization (from the pooled data of four cells) (Fig. 6C-E) (Yanagihara & Irisawa, 1980; DiFrancesco, 1984; DiFrancesco *et al.* 1986).

The time course of both the activation and deactivation of the I_H became slow or

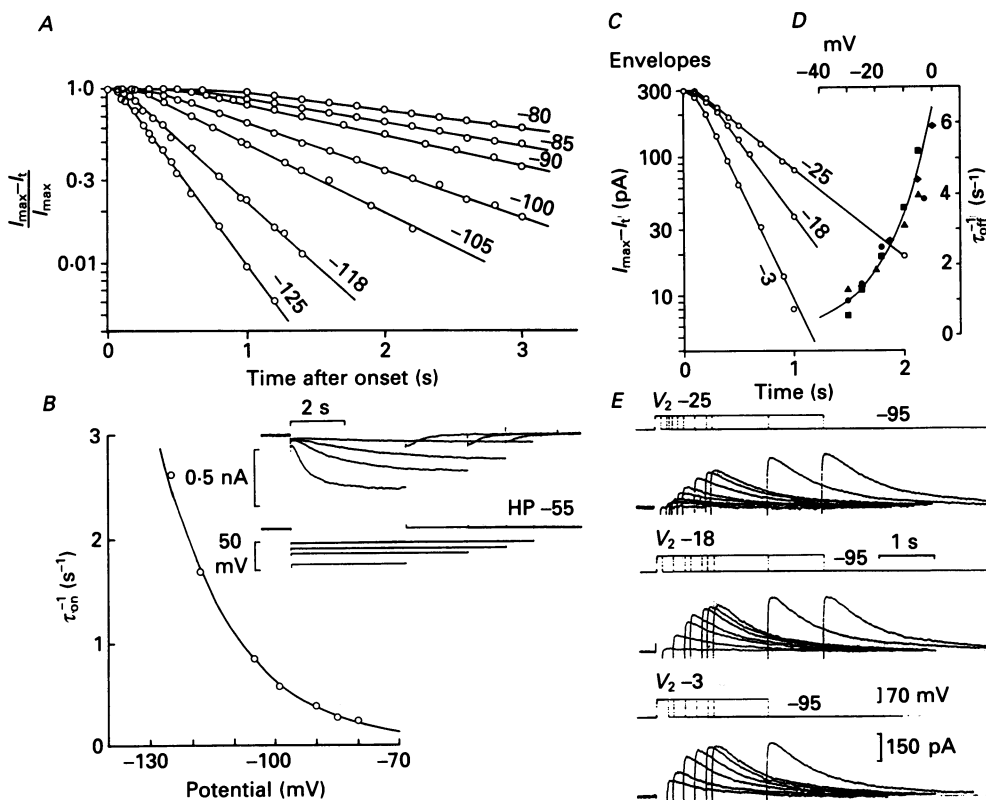


Fig. 6. Time course of I_H . *A* and *B*, time course of the activating I_H . *A*, the ordinate denotes the relative amplitude of I_H ($(I_{\max} - I_t) / I_{\max}$). The abscissa denotes the time after the onset of the hyperpolarizing commands from the holding potential (HP) of -55 mV. *B*, the reciprocal time constant (τ_{on}^{-1}), measured from the data in *A*, is plotted in the ordinate as a function of membrane potential (abscissa). The inset shows sample recordings that were plotted in *A* and *B*. *C-E*, envelope test for the deactivating I_H . The triple-pulse protocol (Mayer & Westbrook, 1983; DiFrancesco, 1986) was adopted in which I_H was activated during the initial hyperpolarizing pulse (V_1 -95 mV). I_H was then briefly (0.1–3 s) deactivated during the second pulse (V_2) at potentials between -40 and zero mV, and finally reactivated at the same voltage as during the initial pulse (V_3 -95 mV). *C*, time course of the envelope of the reactivating I_H (O) as a function of time after the onset of the third pulse. *D*, the reciprocal time constant (τ_{off}^{-1}) determined from results shown in *C* and three other cells. The different symbols represent data from different cells. *E*, sample recordings plotted in *C* showing a reactivating I_H during the third pulse. The HP was -30 mV. The level of the second pulse is indicated beside each envelope (as indicated by V_2).

fast when the temperature at the recording site was decreased by 10°C or increased by 5°C , respectively. In three cells, the Q_{10} between 16 and 26°C was 4.3 ± 0.4 for τ_{on} and 3.6 ± 0.8 for τ_{off} .

Cyclic AMP dependence of I_H

The following sections deal with the possible involvement of a cyclic AMP-dependent intracellular control mechanisms for I_H .

ATP

When ATP was present in the pipettes, I_H had only a moderate ($\leq 15\%$) 'run-down' during the course of the experiments for 2 h ($n > 40$). There was a more rapid 'run-down' of I_H when ATP (5 mM) in the pipette solution was replaced by its non-hydrolysable analogue, β - γ -imidoadenosine-5'-triphosphate (APP(NH)P) (Fig. 7A-C). In three cells, the peak amplitude of I_H was decreased by $92 \pm 6\%$ 35 min after the intracellular dialysis of the cells with APP(NH)P, and this was associated with a hyperpolarizing shift of the half-activation voltage (Fig. 7B). This indicated that the hydrolysable form of ATP was necessary for I_H activation. Bath application of ATP (10 μ M) had no effect on I_H ($n = 3$), whereas ATP (1-10 μ M) reversibly blocked I_M ($n = 5$) (see Akasu, Hirai & Koketsu, 1983).

GTP- γ -S

I_H was progressively activated when GTP- γ -S (300-500 μ M) was present in the pipette solution ($n = 5$) (Fig. 7D and E). The holding current at -50 mV showed a progressive inward shift (1.6 ± 0.2 pA, $n = 5$) associated with a markedly increased conductance. Relaxations on the current trace due to I_H had completely disappeared (Fig. 7E). Both the inward shift of the holding current and the increased conductance were completely reversed when caesium (300 μ M) was added to the 'standard' solution (Fig. 7D and E). These phenomena were never encountered when caesium was added to the superfusate before the rupture of the membrane patch ($n = 2$). The results clearly indicated that GTP- γ -S caused a full activation of I_H . Partial activation of I_H was observed with lower concentrations of GTP- γ -S (30-100 μ M) ($n = 3$). GDP- β -S (300 μ M in the pipettes) had no effect on I_H .

With lower concentrations of GTP- γ -S (3-10 μ M), both I_H and I_M could be recorded in the normal Ringer solution ($n = 4$). Muscarine (3 μ M), luteinizing hormone-releasing hormone (LHRH) (1 μ M) and ATP (3 μ M) produced irreversible block of I_M without significantly affecting I_H ($n = 2$ for each substance) (Adams *et al.* 1982*b*; Akasu *et al.* 1983). The cultured cells were pre-treated with islet-activating protein (IAP) (500 ng ml⁻¹) (Kaken Pharmaceutical) for about 12 h at 4 °C and for another 12 h at 20 °C. Pre-treatment of the cells with IAP did not significantly affect the properties of I_H ($n = 4$) (see DiFrancesco & Tromba, 1987, 1988*b*).

Forskolin

Bath application of forskolin (1-10 μ M) markedly increased the amplitude of I_H between -50 and -130 mV (Fig. 8A-C). The effects of forskolin appeared within 2 min, when the solution containing the drug reached the recording chamber, and disappeared within 30 min after the bath application of the drug was discontinued.

The effect of forskolin (10 μ M) on the steady-state activation curve of I_H was threefold. First, the maximum conductance was clearly increased by $67 \pm 5\%$ ($n = 5$). Second, the half-activation voltage (V_0 in eqn (1)) was shifted from -93.1 ± 0.9 mV

to -83.5 ± 0.6 mV ($n = 3$) (Fig. 8B). In all ten cells tested, forskolin caused an inward shift of the holding current (up to 150 pA) when the holding potential was -60 mV (the bottom of activation curve of I_H in the absence of forskolin). This was always associated with an increased amplitude of an ohmic current at the onset of the

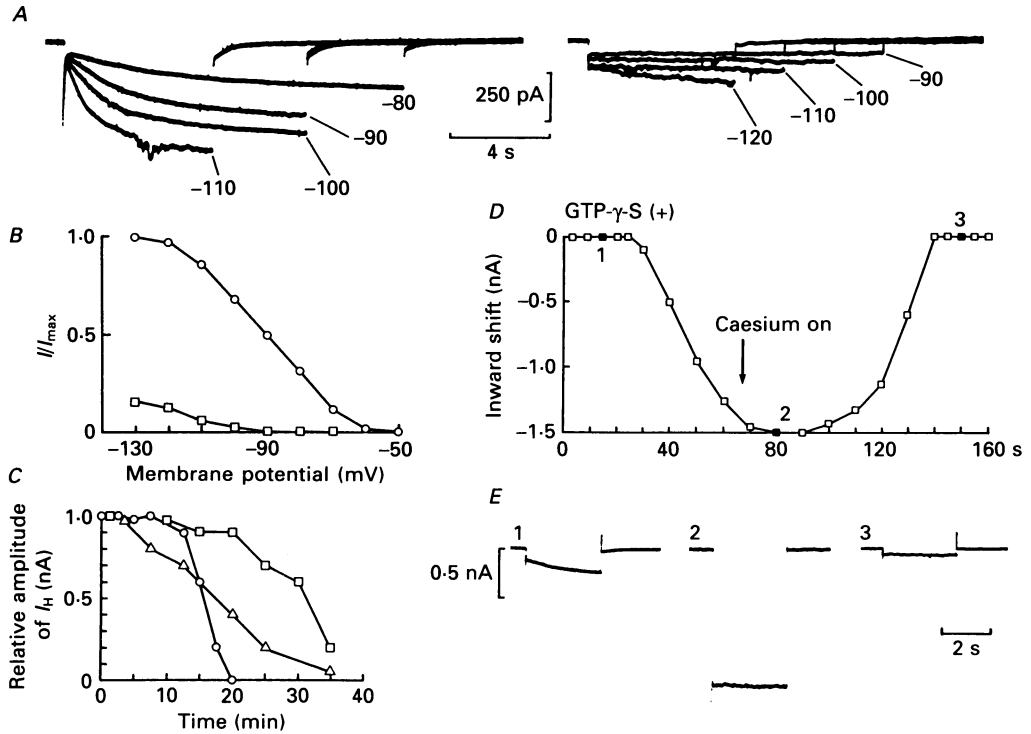


Fig. 7. Effects of APP(NH)P and GTP- γ -S on I_H . *A-C*, the pipette solution contained APP(NH)P (5 mM). The superfusate was changed from the normal Ringer solution to the 'standard' solution 30 s after the establishment of G Ω seal under the cell-attached mode. Approximately 2 min later, the membrane patch was ruptured. This is the starting point of the intracellular dialysis of the cell with APP(NH)P. The holding potential (HP) was -50 mV. *A*, the current traces on the left show a family of I_H at -80 , -90 , -100 and -110 mV (indicated beside each trace). These traces were recorded 0.5–2 min after rupturing the membrane patch. The current traces on the right show I_H at -90 , -100 , -110 and -120 mV (indicated beside each trace). These traces were recorded 20–23 min after rupturing the membrane patch. *B*, the steady-state activation curve of I_H obtained from the same cell as in *A*. \circ , APP(NH)P, 0.5–2 min; \square , APP(NH)P, 20–23 min. *C*, time course of I_H depression with APP(NH)P in three cells (symbols denote different cells). The peak amplitude of the activating I_H at -90 mV was taken as 1.0 in each cell. The abscissa represents the time after time zero. *D* and *E*, the pipette solution contained GTP- γ -S (500 μ M). Time zero was the same as in the experiment with APP(NH)P. *D*, the ordinate denotes an inward shift of the holding current at -50 mV. Caesium (300 μ M) was added to the standard solution at the time indicated by the arrow. The holding current returned to the control. *E*, sample recordings that were plotted in *D*. The command levels were -100 mV. Traces 1–3 correspond to 1–3 in *D* (■).

hyperpolarizing step commands from -60 mV. The inward shift of the holding current was completely reversed when caesium (2 mM) was added to the forskolin-containing standard solution ($n = 4$). The inward shift of the holding current and the

increased ohmic current at the onset of the commands were never seen when the holding potential was between -50 and -40 mV ($n = 7$) (Fig. 8A). Hence, it is suggested that a depolarizing shift in the bottom of the I_H activation curve occurred in the presence of forskolin. Finally, in the presence of forskolin, the time course of the activation of I_H was significantly faster than in the control, but the time course of the deactivation of I_H was markedly slower than in the control (Fig. 8C) (see below).

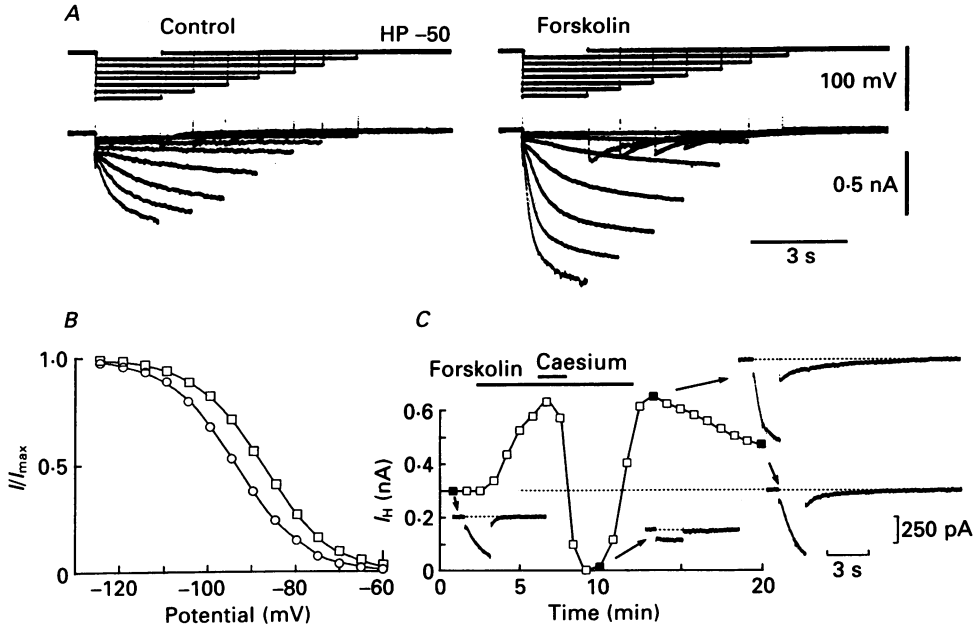


Fig. 8. Effects of forskolin on I_H . *A*, the holding potential (HP) was -50 mV and the cell was subjected to hyperpolarizing commands (10 mV steps from -60 to -120 mV). The traces on the left and right represent I_H in control and in the presence of forskolin ($10 \mu\text{M}$), respectively. *B*, the steady-state activation curve of I_H was obtained from the same cell as in *A*. I_{max} at -130 mV in the presence of forskolin (\square) was taken as 1.0 , and then the control (\circ) curve was scaled up by a factor of 1.6 . The continuous lines denote the relationship in eqn (1). The half-activation voltage (V_0) was shifted from -94 to -88 mV by forskolin. The slope factor was 7.9 mV in control and 7.8 mV in the presence of forskolin. *C*, these are results from another cell. The bath application of forskolin ($10 \mu\text{M}$) is indicated by the bar. Caesium ($300 \mu\text{M}$) was added to the forskolin-containing 'standard' solution for the period of time indicated by the short bar. The ordinate denotes the peak amplitude of the activating I_H at -100 mV (HP was -50 mV). The insets are sample recordings at the times indicated by \blacksquare and arrows.

Forskolin ($10 \mu\text{M}$) also increased the maximum H-conductance in all four IAP-treated cells by $61 \pm 6\%$ implying that the forskolin actions on I_H is independent of the pre-treatment of the cells with IAP.

In the normal Ringer solution, caesium (2 mM) caused $23 \pm 3\%$ ($n = 3$) increase in the amplitude of hyperpolarizing electrotonic potentials evoked by hyperpolarizing current pulses (10 – 15 pA, 500 ms) although caesium did not produce a detectable hyperpolarization. Forskolin ($10 \mu\text{M}$) caused a membrane depolarization (2.3 ± 0.3 mV, $n = 3$) which was associated with a decreased amplitude of hyperpolarizing electrotonic potentials. In three cells, caesium (2 mM) now produced

a membrane hyperpolarization (up to 4 mV) when it was added to the Ringer solution containing forskolin (10 μM).

8-Bromo cyclic AMP and related drugs

Bath application of 8-bromoadenosine 3',5'-cyclic monophosphate (cyclic AMP) (0.1–1 mM) (Fig. 9A) ($n = 5$) and dibutyryl cyclic AMP (1 mM) (Fig. 9B) ($n = 2$) had

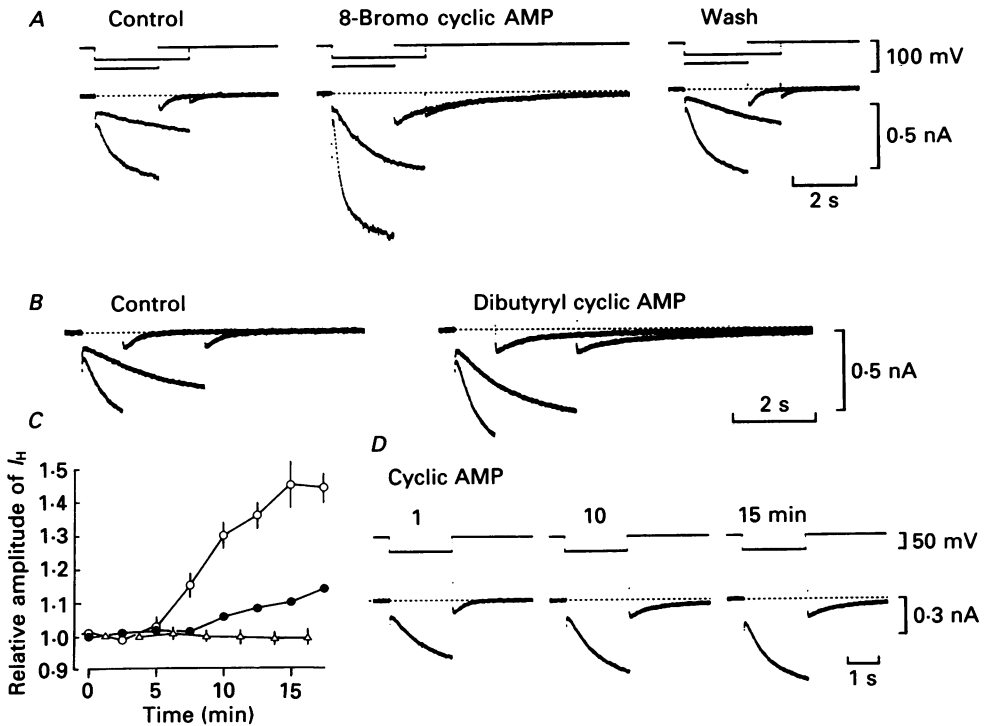


Fig. 9. Effects of cyclic AMP and related drugs on I_H . The holding potential was -50 mV in this figure. *A*, the traces from left to right are I_H (at -90 and -120 mV) in control, in the presence of 8-bromo cyclic AMP (1 mM) and after washing out the drug. *B*, the traces on the left and right are I_H (at -90 and -110 mV) in control and in the presence of dibutyryl cyclic AMP (1 mM). The control I_H was regained 20 min after washing out the drug (not shown). *C*, the effects of intracellular 'loading' with cyclic AMP (3 and 10 μM) and cyclic GMP (10 μM) on I_H are shown. The time zero denotes the rupture of the membrane patch. The relative amplitude of I_H at -90 mV (1.0 at time zero) is plotted in the ordinate. ○ and error bars denote the means \pm s.e.m. for 10 μM -cyclic AMP ($n = 3$). Similarly, △ and error bars represent the results with 10 μM -cyclic GMP ($n = 3$). ● denote the results with 3 μM -cyclic AMP in one cell. *D*, sample recordings, plotted in *C*, showing that I_H (1 min after time zero, left) was increased by 36% (middle) and by 44% (right), 10 and 20 min, after cyclic AMP 'loading', respectively. The pipette solution contained cyclic AMP (10 μM).

essentially the same effects on I_H as forskolin, except the onsets of drug actions were slower, reaching the maximum level only 15–20 min after drug application. 8-Bromo cyclic AMP (1 mM) increased the maximum H-conductance by $59 \pm 6\%$ ($n = 3$). I_H returned to the control amplitude within 40 min after the bath application of the drugs was discontinued. Intracellular loading with cyclic AMP (3–10 μM) induced a

progressive increase in the peak amplitude of I_H in four cells. The peak amplitude of I_H at -100 mV was increased by $45.0 \pm 6.5\%$ ($n = 3$), 15 min after the 'rupture' of the membrane patch (17% increase after 20 min with $3 \mu\text{M}$ -cyclic AMP; $n = 1$) (Fig. 9C and D). Guanosine 3',5'-cyclic monophosphate (cyclic GMP) ($10 \mu\text{M}$) failed to facilitate I_H in all of three cells (Fig. 9C).

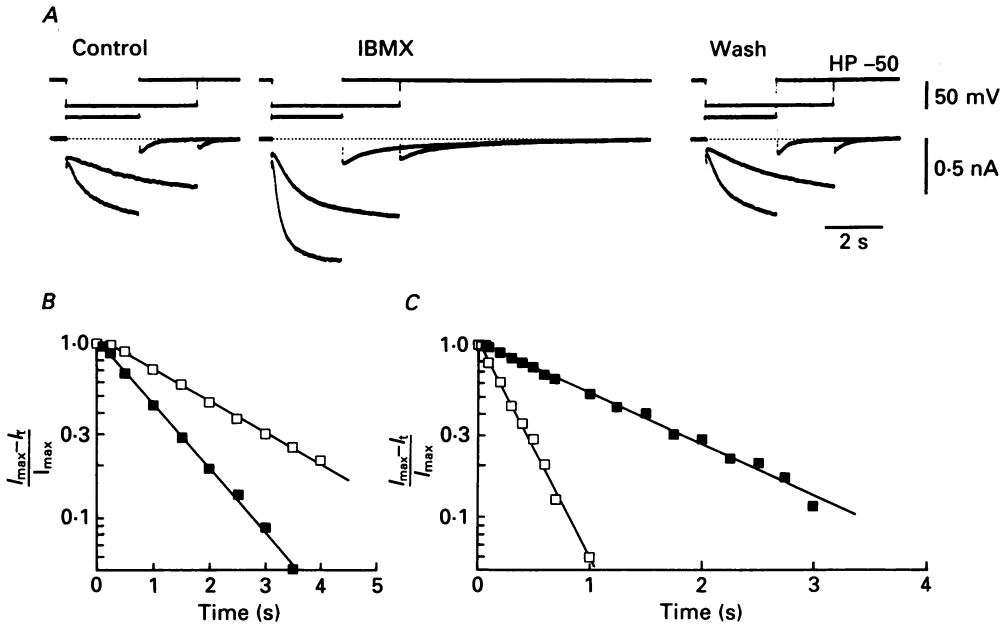


Fig. 10. Effects of IBMX on I_H . These results were obtained from a single cell at a holding potential (HP) of -50 mV. *A*, the traces from left to right denote I_H (at -95 and -115 mV) in control, in the presence of IBMX (1 mM) and after washing out the drug. *B*, the activating time course of I_H at -95 mV had a τ_{on} of 2.8 s in control (\square) and 1.3 s in the presence of IBMX (\blacksquare). *C*, the deactivating time course of I_H at -50 mV had a τ_{off} of 400 ms in control (\square) and 1500 ms in the presence of IBMX (\blacksquare).

Phosphodiesterase inhibitor

The phosphodiesterase inhibitor, 3-isobutyl-1-methylxanthine (IBMX) (0.1 – 1 mM), also induced forskolin-like effects on the steady-state activation curve of I_H and the time course of I_H ($n = 6$) (Fig. 10A). IBMX (1 mM) increased the maximum H-conductance by $63 \pm 4\%$ ($n = 5$). The onset of drug action was comparable to that of 8-bromo cyclic AMP, but I_H returned to its respective control during a 10 min wash-out with 'standard' solution.

It was clear from the results shown in Figs 8–10 that the time course of I_H was significantly changed by forskolin, cyclic AMP and IBMX, indicating that a shift of the voltage dependence of activation and deactivation of I_H occurred in the presence of these drugs. Therefore, the effects of IBMX (1 mM) on the time constant of both activation (τ_{on}) and deactivation (τ_{off}) of I_H were studied. τ_{on} was reduced approximately in half and τ_{off} was increased three or more times by IBMX ($n = 3$) (Fig. 10B and C). Essentially the same results were obtained with forskolin ($10 \mu\text{M}$)

($n = 3$) and 8-bromo cyclic AMP (1 mM) ($n = 3$). These observations were compatible with a depolarizing shift of the voltage dependence of activation and deactivation kinetics of I_H (shown in Fig. 6).

Protein kinase inhibitors

H-8 (1–10 μM) decreased the amplitude of I_H by as much as 40% ($26 \pm 4\%$, $n = 5$) (Fig. 11A). The depression of I_H was observed after bath application of H-8 for

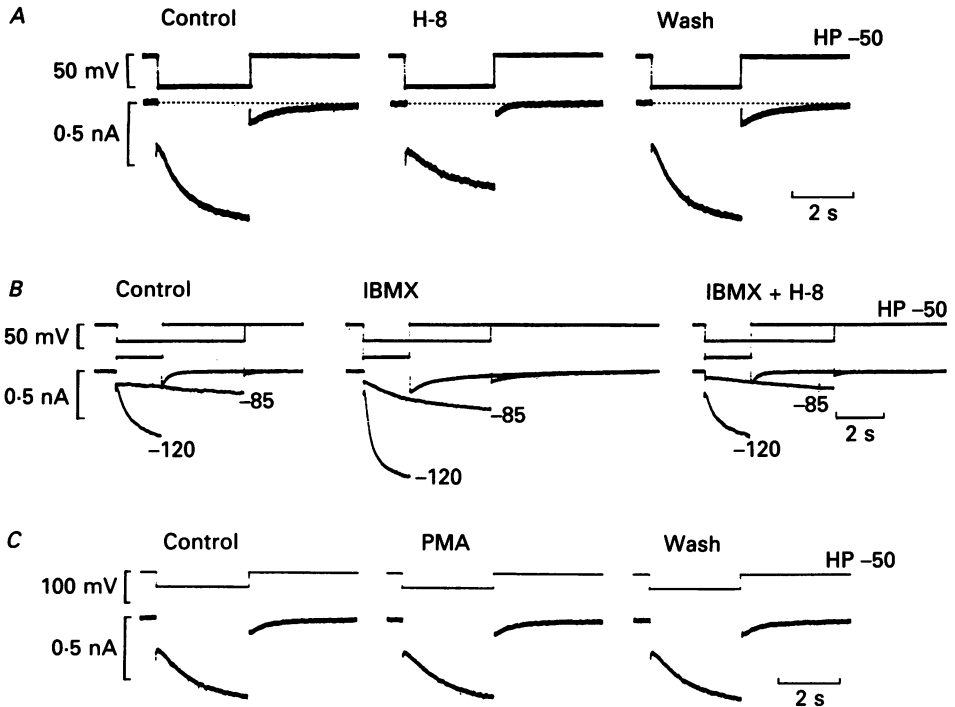


Fig. 11. Effects of H-8 and PMA on I_H . The results were obtained from three different cells. The holding potential (HP) was -50 mV. *A*, H-8 ($3 \mu\text{M}$) depressed the amplitude of I_H at -100 mV by approximately 40%. *B*, H-8 ($3 \mu\text{M}$) reversed the enhancement of I_H amplitude at -85 and -120 mV by IBMX (1 mM). The traces on the left are the control for both IBMX (middle traces) and IBMX plus H-8 (traces on the right). *C*, PMA ($3 \mu\text{M}$) had no effect on I_H at -100 mV.

20–30 min. H-8 ($3 \mu\text{M}$) was also effective when I_H had already been facilitated by forskolin (1 μM) ($n = 2$) or by IBMX (1 mM) ($n = 1$; Fig. 11B). On the other hand, phorbol 12-myristate 13-acetate (PMA) (10 μM), a potent activator of C kinase (Castagna, Takai, Kaibuchi, Sano, Kikkawa & Nishizuka, 1982), was without effect on I_H ($n = 3$; Fig. 11C), while PMA (10 μM) depressed I_M by about 35% in three cells.

DISCUSSION

The present study has demonstrated a hyperpolarization-activated sodium-potassium current (I_H) that can be regulated by the basal activity of adenylate cyclase in bull-frog sympathetic ganglion cells in primary culture. The final step in

coupling between adenylate cyclase and the cation channels may involve a cyclic AMP-dependent protein kinase (A-kinase).

Properties of I_H

The activation and deactivation kinetics of I_H , including the high Q_{10} of the time course, in bull-frog sympathetic neurones (Figs 1–6) are quite similar to those reported for other nerve and muscle cells, such as dorsal root ganglion cells (I_h), hippocampal pyramidal cells (I_Q), cardiac pacemaker cells (I_f – I_h) and gut smooth muscle cells (Yanagihara & Irisawa, 1980; DiFrancesco, 1981*a, b*; Halliwell & Adams, 1982; Mayer & Westbrook, 1983; Benham, Bolton, Denbigh & Lang, 1987).

Previous studies in cultured rat DRG neurones have led to speculation that the resting membrane potential may be determined by counter-balancing two voltage-dependent conductances (Mayer & Westbrook, 1983; Mayer, 1986). One is I_H exerting the depolarizing influence (Fig. 12*A* and *B*) and the other is a non-inactivating outward current exerting the hyperpolarizing influence. Although direct evidence is still lacking, I_M has been thought of as one of the suitable candidates (see Mayer, 1986). The results in the present study have shown that the bottom of the I_H activation curve was near -60 mV and -50 mV in the absence and presence of forskolin, respectively. The bottom of the activation curve of I_M was -64 ± 1 mV ($n = 40$) (Adams *et al.* 1982*a*) and this value was not altered by $10 \mu\text{M}$ -forskolin (T. Tokimasa, unpublished observation). These observations indicated that the steady-state I_H activation curve overlaps with that of I_M between -50 and -64 mV in the presence of forskolin. Therefore, under certain conditions, I_H and I_M may very well balance at the resting potential in bull-frog sympathetic neurones. The depolarizing influence of I_H may be significant physiologically when the cells are strongly hyperpolarized with respect to rest (e.g. during the after-hyperpolarization following the spike). However, these speculations should be proved experimentally by further experiments.

Cyclic AMP-dependent facilitation of I_H

It has been shown that the hydrolysable form of ATP is necessary for I_H activation. This indicates that ATP functions either as a direct energy source for the cation channels, or as a substrate for cyclic AMP formation by adenylate cyclase. In either case the high Q_{10} of both τ_{on} and τ_{off} of I_H is to be expected. It is unlikely that the presence of I_H in the whole-cell configuration resulted from some kind of pathological 'loading' of ATP from the pipette solution, since I_H could be clearly recorded with conventional microelectrode methods (Fig. 12*C*).

A previous study by Tsien, Giles & Greengard (1972) has indicated that cyclic AMP mediates the effects of adrenaline on a pacemaker current in cardiac Purkinje fibres (I_{K2} , now called I_f). Recent studies in rabbit sino-atrial node cells have demonstrated that acetylcholine (ACh) acting at muscarinic receptors causes a hyperpolarizing shift in the steady-state activation curves of I_f and thereby inhibits the peak amplitude of the current near the half-activation voltage (DiFrancesco & Tromba, 1987, 1988*a, b*). Adrenaline, acting at β -adrenoceptors, causes a depolarizing shift in the I_f activation curve (DiFrancesco *et al.* 1986). Both ACh and adrenaline regulate the basal activity of adenylate cyclase and hence the cytosolic concentration of cyclic AMP.

Three lines of evidence in the present study show that cyclic AMP also regulates I_H in nerve cells. First, an adenylate cyclase activator, forskolin, increased the peak amplitude of I_H . Second, both intracellular 'loading' of cyclic AMP and bath application of membrane permeable cyclic AMP analogues mimicked the forskolin

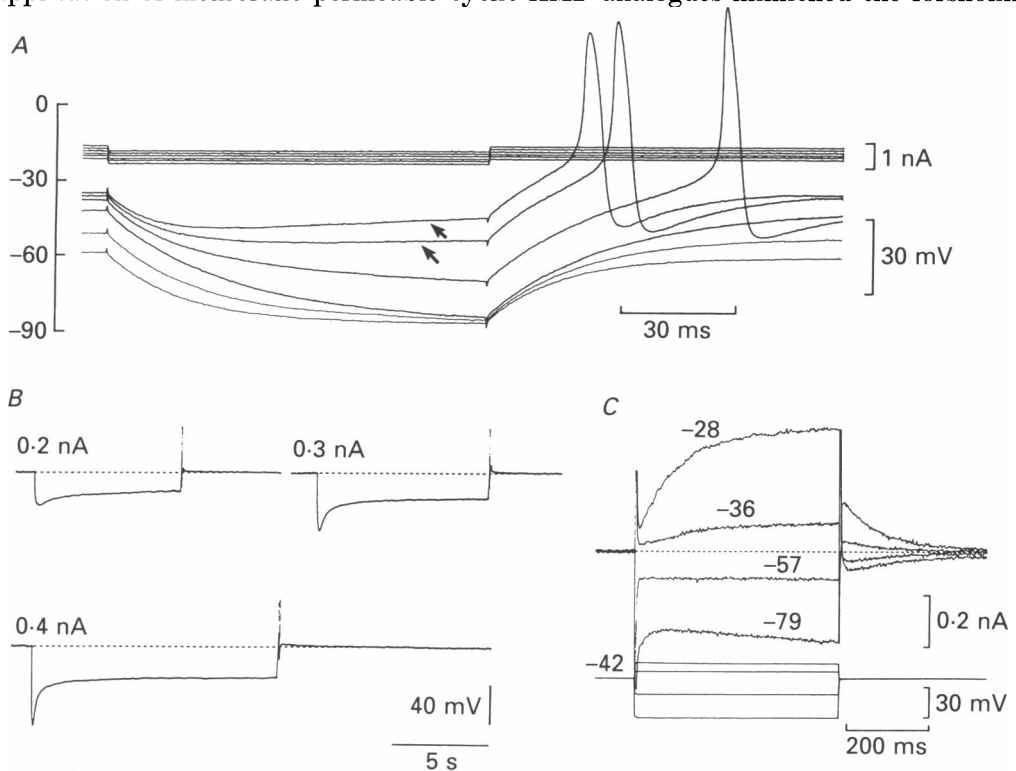


Fig. 12. Potential clamping of I_H studied with conventional microelectrode methods. The results were obtained from a single cell superfused with a potassium-rich (7 mM) Ringer solution. The resting potential was -38 mV. The cell membrane was polarized by passing current pulses or continuous DC through the recording electrode. *A*, hyperpolarizing electrotonic potentials were evoked by current pulses (200 pA, 100 ms) at various membrane potentials (DC was applied in 100 pA steps from -38 mV). At depolarized levels with respect to the resting potential, deactivation of I_M resulted in a depolarizing sag of the electrotonic potentials (indicated by arrows). At hyperpolarized levels, the input resistance became progressively smaller with conditioning hyperpolarization. *B*, the depolarizing sag of the electrotonic potentials due to I_H activation are shown. Prolonged (7–15 s) hyperpolarizing current pulses (0.2, 0.3 and 0.4 nA indicated beside each tonic potential) were applied from -38 mV. *C*, I_H and I_M were studied with a single-electrode voltage clamp (switching frequency was 5 kHz). The holding potential was -42 mV and the command levels are indicated beside each current trace. The deactivating I_M was followed by an activating I_H . TTX ($3 \mu\text{M}$) was present in *C*.

actions. Third, the phosphodiesterase inhibitor, IBMX, also mimicked the forskolin actions. The results in the present study did not allow us to explain the difference between the wash-out time of forskolin actions and IBMX actions on I_H . It might be that adenylate cyclase, when stimulated by forskolin, returns to its basal activity with prolonged time course or that forskolin decreases the stimulatory actions on

adenylate cyclase with slow time course. Establishment of an intracellular perfusion technique may allow us to answer this question.

The forskolin actions on I_H were comparable to those observed on I_f . As in cardiac cells, forskolin caused a depolarizing shift in both the steady-state activation curve and the voltage dependence of I_H kinetics (speeding up of τ_{on} and slowing down of τ_{off}). In this context, results from a recent study in *Bufo* smooth muscle cells (Sims, Singer & Walsh, 1988) are of some interest. They showed that the cyclic AMP-mediated augmentation of I_M by β -agonists was associated with a significant slowing of the reactivation time course of I_M , implying a displacement of the voltage dependence of the activation kinetics of I_M (Adams *et al.* 1982*a*).

The main difference between forskolin actions on I_f and I_H is that forskolin does not increase the amplitude of I_f at the top of the activation curve, whereas it clearly does for I_H (Fig. 8). This indicates that forskolin actions in sympathetic neurones are distinct from those in cardiac cells. An upward shift in the activation curve of I_H indicates that forskolin increases either the total number of H-channels, which are not available in the absence of forskolin, or it increases the single-channel conductance. The present study did not address this question and further experiments are needed to measure single-channel conductances.

Involvement of protein kinase A in I_H regulation

Recent studies in bull-frog sympathetic neurones have shown that ACh blocks I_M by activating an IAP-insensitive G protein (Pfaffinger, 1988) and increasing the subsequent turnover of phosphatidylinositol (Dutar & Nicoll, 1988; Pfaffinger, Leibowitz, Subers, Nathanson, Almers & Hille, 1988). Protein kinase C (Castagna *et al.* 1982) has been proposed as a second messenger (Tsuji, Minota & Kuba, 1987). It seems unlikely that cyclic AMP mediates the muscarinic actions (see Brown, 1988). The results in the present study clearly indicate that at least two distinct intracellular control mechanisms co-exist in a single cell (one for I_M and the other for I_H). However, further experiments are necessary to identify the receptor agonists which regulate I_H via the cyclic AMP-dependent mechanism. So far, these do not include ATP, muscarine and LHRH, all of which blocked I_M . Isoproterenol ($3 \mu\text{M}$) was without effect on I_H ($n = 4$), which also blocks I_M (Akasu, 1988, 1989).

Three lines of evidence in the present study have suggested that protein kinase A may be involved in I_H regulation. First, PMA ($10 \mu\text{M}$) failed to enhance I_H , whereas PMA reduced the amplitude of I_M (Pfaffinger *et al.* 1988 and the present study). Second, H-8 ($1\text{--}3 \mu\text{M}$) clearly reduced the amplitude of I_H , indicating that the protein kinase inhibitor blocked A kinase (Hidaka, Inagaki, Kawamoto & Sasaki, 1984). Third, the enhancement in I_H amplitude by both forskolin and IBMX was completely reversed by H-8 (Fig. 11*B*).

In conclusion, the present study has demonstrated for the first time the presence of an inward rectifying sodium-potassium current in bull-frog sympathetic neurones. The results also show that the current can be regulated by the basal activity of adenylate cyclase, presumably through a cyclic AMP-dependent protein kinase. A cation current with properties similar to I_H that is also regulated by a cyclic AMP-dependent mechanism has been observed not only in cultured bull-frog dorsal root

ganglion cells (T. Tokimasa, unpublished data) but also in cultured rat dorsal root ganglion cells (T. Tokimasa & K. Sugiyama, unpublished data). This may support our proposal that cyclic AMP could regulate the membrane excitability in vertebrate nerve cells.

This work was supported by a Grant-in-Aid for Scientific Research from the Ministry of Education, Science and Culture of Japan and the Naito Foundation (code 87-128). The authors would like to thank Mr Kuwahara for assistance with the least-squares method for fitting the activation curve of I_H .

REFERENCES

- ADAMS, P. R., BROWN, D. A. & CONSTANTI, A. (1982*a*). M-currents and other potassium currents in bullfrog sympathetic neurones. *Journal of Physiology* **330**, 537-572.
- ADAMS, P. R., BROWN, D. A. & CONSTANTI, A. (1982*b*). Pharmacological inhibition of the M-current. *Journal of Physiology* **332**, 223-262.
- AKASU, T. (1988). Adrenaline depolarization in paravertebral sympathetic neurones of bullfrogs. *Pflügers Archiv* **411**, 80-87.
- AKASU, T. (1989). Adrenaline inhibits muscarinic transmission in bullfrog sympathetic ganglia. *Pflügers Archiv* **413**, 616-621.
- AKASU, T., HIRAI, K. & KOKETSU, K. (1983). Modulatory actions of ATP on membrane potentials of bullfrog sympathetic ganglion cells. *Brain Research* **258**, 313-317.
- BARRETT, E. F., BARRETT, J. N. & CRILL, W. E. (1980). Voltage-sensitive outward currents in cat motoneurons. *Journal of Physiology* **304**, 251-276.
- BENHAM, C. D., BOLTON, T. B., DENBIGH, J. S. & LANG, R. J. (1987). Inward rectification in freshly isolated single smooth muscle cells of the rabbit jejunum. *Journal of Physiology* **383**, 461-476.
- BROWN, D. (1988). M-currents: an update. *Trends in Neurosciences* **11**, 294-299.
- CASTAGNA, M., TAKAI, Y., KAIBUCHI, K., SANO, K., KIKKAWA, U. & NISHIZUKA, Y. (1982). Direct activation of calcium-activated, phospholipid-dependent protein kinase by tumor-promoting phorbol esters. *Journal of Biological Chemistry* **257**, 7847-7851.
- CREPEL, F. & PENIT-SORIA, J. (1986). Inward rectification and low threshold calcium conductance in rat cerebellar Purkinje cells an *in vitro* study. *Journal of Physiology* **372**, 1-23.
- DI FRANCESCO, D. (1981*a*). A new interpretation of the pace-maker current in calf Purkinje fibres. *Journal of Physiology* **314**, 359-376.
- DI FRANCESCO, D. (1981*b*). A study of the ionic nature of the pace-maker current in calf Purkinje fibres. *Journal of Physiology* **314**, 377-393.
- DI FRANCESCO, D. (1984). Characterization of the pace-maker current kinetics in calf Purkinje fibres. *Journal of Physiology* **348**, 341-367.
- DI FRANCESCO, D., FERRONI, A., MAZZANTI, M. & TROMBA, C. (1986). Properties of the hyperpolarizing-activated current (i_t) in cells isolated from the rabbit sino-atrial node. *Journal of Physiology* **377**, 61-88.
- DI FRANCESCO, D. & TROMBA, C. (1987). Acetylcholine inhibits activation of the cardiac hyperpolarizing-activated current, i_t . *Pflügers Archiv* **410**, 139-142.
- DI FRANCESCO, D. & TROMBA, C. (1988*a*). Inhibition of the hyperpolarization-activated current (i_t) induced by acetylcholine in rabbit sino-atrial node myocytes. *Journal of Physiology* **405**, 477-491.
- DI FRANCESCO, D. & TROMBA, C. (1988*b*). Muscarinic control of the hyperpolarization-activated current (i_t) in rabbit sino-atrial node myocytes. *Journal of Physiology* **405**, 493-510.
- DODD, J. & HORN, J. P. (1983). A reclassification of B and C neurones in the ninth and tenth paravertebral sympathetic ganglia of the bullfrog. *Journal of Physiology* **334**, 255-269.
- DUTAR, P. & NICOLL, R. A. (1988). Stimulation of phosphatidylinositol (PI) turnover may mediate the muscarinic suppression of the M-current in hippocampal pyramidal cells. *Neuroscience Letters* **85**, 89-94.
- FOX, A. P., NOWYCKY, M. C. & TSIEN, R. W. (1987). Kinetic and pharmacological properties distinguishing three types of calcium currents in chick sensory neurones. *Journal of Physiology* **394**, 149-172.

- GRIFFITH, W. H. (1988). Membrane properties of cell types within guinea pig basal forebrain nuclei *in vitro*. *Journal of Neurophysiology* **59**, 1590–1612.
- HALLIWELL, J. V. & ADAMS, P. R. (1982). Voltage-clamp analysis of muscarinic excitation in hippocampal neurons. *Brain Research* **250**, 71–92.
- HIDAKA, H., INAGAKI, M., KAWAMOTO, S. & SASAKI, Y. (1984). Isoquinolinesulfonamides, novel and potent inhibitors of cyclic nucleotide dependent protein kinase and protein kinase C. *Biochemistry* **23**, 5036–5041.
- JONES, S. W. (1987a). Sodium currents in dissociated bull-frog sympathetic neurones. *Journal of Physiology* **389**, 605–627.
- JONES, S. W. (1987b). GTP- γ -S inhibits the M-current of dissociated bullfrog sympathetic neurons. *Society for Neuroscience Abstracts* **13**, 533.
- KUFFLER, S. W. & SEJNOWSKI, T. J. (1983). Peptidergic and muscarinic excitation at amphibian sympathetic synapses. *Journal of Physiology* **341**, 257–278.
- MAYER, M. L. (1986). Selective block of inward but not outward rectification in rat sensory neurones infected with herpes simplex virus. *Journal of Physiology* **375**, 327–338.
- MAYER, M. L. & WESTBROOK, G. L. (1983). A voltage-clamp analysis of inward (anomalous) rectification in mouse spinal sensory ganglion neurones. *Journal of Physiology* **340**, 19–45.
- PENNEFATHER, P., LANCASTER, B., ADAMS, P. R. & NICOLL, R. A. (1985). Two distinct Ca-dependent K currents in bullfrog sympathetic ganglion cells. *Proceedings of the National Academy of Sciences of the USA* **82**, 3040–3044.
- PFÄFFINGER, P. (1988). Muscarine and t-LHRH suppress M-current by activating an IAP-insensitive G-protein. *Journal of Neuroscience* **8**, 3343–3353.
- PFÄFFINGER, P. J., LEIBOWITZ, M. D., SUBERS, E. M., NATHANSON, N. M., ALMERS, W. & HILLE, B. (1988). Agonists that suppress M-current elicit phosphoinositide turnover and Ca²⁺ transients, but these events do not explain M-current suppression. *Neuron* **1**, 477–484.
- SIMS, S. M., SINGER, J. J. & WALSH, J. V. (1988). Antagonistic adrenergic–muscarinic regulation of M current in smooth muscle cells. *Science* **239**, 190–193.
- TANAKA, K. & KUBA, K. (1987). The Ca²⁺-sensitive K⁺-currents underlying the slow after-hyperpolarization of bullfrog sympathetic neurones. *Pflügers Archiv* **410**, 234–242.
- TOKIMASA, T. (1984). Calcium-dependent hyperpolarizations in bullfrog sympathetic neurons. *Neuroscience* **12**, 929–937.
- TOKIMASA, T. (1985a). Intracellular Ca²⁺-ions inactivate K⁺-current in bullfrog sympathetic neurons. *Brain Research* **337**, 386–391.
- TOKIMASA, T. (1985b). Spontaneous muscarinic suppression of the Ca-activated K-current in bullfrog sympathetic neurons. *Brain Research* **344**, 134–141.
- TOKIMASA, T., AKASU, T., NISHIMURA, T. & TSURUSAKI, M. (1989). Voltage-dependent cation current in cultured bullfrog sympathetic ganglion cells. *Neuroscience Research*, suppl. **9**, 77.
- TSIEN, R. W., GILES, W. & GREENGARD, P. (1972). Cyclic AMP mediates the effects of adrenaline on cardiac Purkinje fibres. *Nature* **240**, 181–183.
- TSUJI, S., MINOTA, S. & KUBA, K. (1987). Regulation of two ion channels by a common muscarinic receptor-transduction system in a vertebrate neuron. *Neuroscience Letters* **81**, 139–145.
- WILLIAMS, J. T., COLMERS, W. F. & PAN, Z. Z. (1988a). Voltage- and ligand-activated inwardly rectifying currents in dorsal raphe neurons *in vitro*. *Journal of Neuroscience* **8**, 3499–3506.
- WILLIAMS, J. T., NORTH, R. A. & TOKIMASA, T. (1988b). Inward rectification of resting and opiate-activated potassium currents in rat locus coeruleus neurons. *Journal of Neuroscience* **8**, 4299–4306.
- YANAGIHARA, K. & IRISAWA, H. (1980). Inward current activated during hyperpolarization in the rabbit sinoatrial node cell. *Pflügers Archiv* **385**, 11–19.